The farnesyltransferase inhibitor R115777 (ZARNESTRA®) enhances the pro-apoptotic activity of interferon-α through the inhibition of multiple survival pathways

ARTICLE *in* INTERNATIONAL JOURNAL OF CANCER · NOVEMBER 2007

Impact Factor: 5.09 · DOI: 10.1002/ijc.22964 · Source: PubMed

Int. J. Cancer: **121,** 2317–2330 (2007)

The farnesyltransferase inhibitor R115777 (ZARNESTRA®) enhances the pro-apoptotic activity of interferon-α through the inhibition of multiple survival pathways

Michele Caraglia[1]*, Monica Marra[1], Caterina Viscomi[2,3], Anna Maria D'Alessandro[4], Alfredo Budillon[1], Giuseppina Meo[1], Claudio Arra[5], Antonio Barbieri[5], Ulf R Rapp[6], Alfonso Baldi[4], Pierfrancesco Tassone[2,3], Salvatore Venuta[2,3], Alberto Abbruzzese[4]* and Pierosandro Tagliaferri[2,3]

[1]*Experimental Pharmacology Unit, Experimental Oncology Department, National Cancer Institute Fondazione "G. Pascale", Naples, Italy*
[2]*Department of Experimental and Clinical Medicine, University Magna Grécia of Catanzaro, Catanzaro. Italy*
[3]*Oncology Center "Germaneto", Catanzaro, Italy*
[4]*Department of Biochemistry and Biophysics, II University of Naples, Naples, Italy*
[5]*Experimental Oncology Department, Animal Facility, National Cancer Institute Fondazione "G. Pascale", Naples, Italy*
[6]*Institute of Medical Radiation and Cell Research (MSZ), University of Würzburg, 97078 Würzburg, Germany*

Interferon α (IFNα) induces an EGF-Ras→Raf-1→Erk dependent survival pathway counteracting apoptosis induced by the cytokine. In this paper we have evaluated the effects of the combination between farnesyl-transferase inhibitor (FTI) R115777 and IFNα on the growth inhibition and apoptosis of cancer cells. Simultaneous exposure to R115777 and IFNα produced synergistic both antiproliferative and proapoptotic effects. In these experimental conditions, IFNα and R115777 completely antagonized the increased activity of both Ras and Erk-1/2 induced by IFNα and strongly reduced Akt activity. Furthermore, treatment with R115777 in combination with IFNα regimen induced tumor growth delay on established KB cell xenografts in nude mice, while the single agents were almost inactive. R115777 was again able to antagonize the Ras-dependent survival pathway induced by IFNα also *in vivo*. Raf-1, one of the downstream targets of Ras, has been reported to activate bcl-2 through displacement and/or phosphorylation of Bad. We have found that IFNα induced mitochondrial localization of Raf-1 that was antagonized by R115777. Moreover, IFNα increased Raf-1/bcl-2 immuno-conjugate formation and intracellular co-localization and enhanced phosphorylation of Bad at Ser 112 and again R115777 counteracted all these effects. Moreover, the use of plasmids encoding for dominant negative or dominant positive Raf-1 antagonized and potentiated, respectively, the co-immunoprecipitation between Raf-1 and bcl-2. In conclusion, FTI R115777 strongly potentiates the antitumor activity of IFNα both *in vitro* and *in vivo* through the inhibition of different survival pathways that are dependent from isoprenylation of intracellular proteins such as ras.

Key words: farnesyl transferase inhibitor; interferon α; epidermoid cancer; apoptosis; Ras

R115777 is a potent and selective nonpeptidomimetic competitive farnesyl-transferase inhibitor (FTI) with antitumor activity as reported by several *in vitro* and *in vivo* studies.[1,2] R115777 has displayed the most interesting activity in hematologic neoplasms with a schedule based on oral administration twice a day for 3 consecutive weeks with a week of rest.[3] Although R115777 has been initially developed as Ras inhibitor, it is now clear that antitumor activity of R115777 may be correlated to the effects on a variety of proteins that require posttranslational modifications by prenylation.[4]

IFNα is a cytokine with pleiotropic biological activity mediated by the activation of intracellular pathways after binding to a specific surface receptor.[5] Although IFNα has clearly shown antitumor activity, the mechanism of such effects remains at the present mostly undefined. Direct antitumor activity as well as immunostimulatory and antiangiogenic activity have been described in a variety of experimental systems.[6,7] IFNα has been widely used in the therapy of several neoplasms, including epidermoid cancer of head and neck[8–11]; however, contrasting data have generated concerns regarding the clinical effectiveness of IFNα used as single agent in solid tumors. In fact, the benefit of IFNα treatment is limited to some neoplasms[12,13] and mechanisms of tumor resistance to IFNα have been extensively described.[14] In this regard, we have shown that IFNα, at growth inhibitory concentrations, enhances the expression and signaling activity of the EGF-R in epidermoid cancer cell lines.[15–17] We have speculated that the enhanced expression and function of EGF-R in tumor cells could represent a stress response that is activated to provide an escape mechanism to the growth inhibition induced by IFNα.[17,18] In fact, EGF causes a protective response in tumor cells against IFNα-induced apoptosis that occurs through the triggering of a stress kinase pathway.[19] It is well known that EGF acts through the binding to its specific receptor, EGF-R, a transmembrane protein with a cytoplasmic tyrosine kinase domain.[20,21] The phosphorylation of its intra-cytoplasmic tail allows the interaction of EGF-R with cytoplasmic factors that can induce Ras activation only when Ras is isoprenylated and, therefore, linked to the inner side of the cell membrane. In fact, the latter event allows its interaction for co-localization with EGF-R-associated nucleotide exchange factors that favor GTP:GDP exchange and the subsequent Ras activation. The stimulation of Ras induces the triggering of several antiapoptotic and proliferative pathways such as the mitogen activated protein kinase (MAPK) cascade.[20–23] A second important antiapoptotic pathway regulated by EGF and Ras is the signaling *via* Akt/PKB.[24,25] We have also reported that a specific hyperactivation of EGFR-dependent Ras/Erk-1/2 pathway counteracts IFNα-mediated apoptosis.[17] All these observations suggested to us that the selective targeting of this survival pathway might enhance the antitumor activity of IFNα. In fact, either the transfection of a dominant form of Ras RASN17 or the treatment of tumor cells with a specific MEK1 inhibitor (PD098056) strongly strengthened the apoptosis induced by IFNα.[17] All these findings suggest that epidermoid tumor cells counteract the IFNα-induced apoptosis

Grant sponsor: MIUR Rome; Grant number: PRIN 2005; Grant sponsor: Associazione Italiana Ricerca sul Cancro (AIRC); Grant sponsor: Italian Ministry of Health; Grant numbers: FSN 2004, FSN 2005; Grant sponsor: Centro Regionale di Competenza di "Diagnostica e Farmaceutica Molecolari" of Regione Campania.

***Correspondence to:** Department of Biochemistry and Biophysics, II University of Naples, Via Costantinopoli No. 16, 80138 Naples, Italy. Fax: +39-081-5665863. E-mail: alberto.abbruzzese@unina2.it or Experimental Pharmacology Unit, Experimental Oncology Department, National Cancer Institute Fondazione "G. Pascale", Via Mariano Semmola, 80131 Naples, Italy. Fax: +39-0815903813.
E-mail: michele.caraglia@fondazionepascale.it

Received 22 September 2006; Accepted after revision 6 June 2007
DOI 10.1002/ijc.22964
Published online 26 July 2007 in Wiley InterScience (www.interscience.wiley.com).

through a survival pathway that involves the hyper-activation of the EGF-dependent Ras→Erk signaling.[17]

In the present paper, we have investigated the pharmacological interactions on apoptosis and growth inhibition between IFNα and the FTI R115777 in order both to reduce R115777 concentration required for the antitumor activity and to overcome the described mechanisms of cell resistance to IFNα. We have indeed found a strong synergistic antitumor activity both *in vitro* and *in vivo*. Therefore, we have characterized the molecular targets of R115777 and the interaction with the EGF-dependent signaling and we have specifically investigated the effect induced by the synergistic combination of R115777 and IFNα on the Akt and Erk survival pathways. Moreover, our results show that FTI R115777 blocks the functional interaction between Raf-1-dependent pathway and bcl-related proteins allowing the occurrence of the apoptotic process.

Material and methods

Materials

DMEM, BSA and FBS were purchased from Flow Laboratories (Milan, Italy). Tissue culture plasticware was from Becton Dickinson (Lincoln Park, NJ). R115777 was a gift of Orthobiotech (Janssen Research Center, Titusville, NJ). Interferon α-2b recombinant was a gift of Schering (Schering-Plough, NJ). Protein Sepharose A was purchased from Sigma (St. Louis, MO). Rabbit antisera raised against α-tubulin, GAPDH, pErk-1 K-23, Erk C-14 and Bcl-2 C-2 MAbs were purchased from Santa Cruz Biotechnology (Santa Cruz, CA). Anti-Akt MAb, the relative activity evaluation kit, rabbit 9291 antiserum raised against Ser 112 of Bad and 9292 rabbit antiserum raised against total Bad were purchased by Cell Signalling (Cell Signaling Technology, MA). Anti-pan-Ras clone 10 MAb was purchased from Calbiochem (Darmstadt, Germany).

Cell culture

The human oropharyngeal epidermoid carcinoma KB and lung H13555 cancer cell lines, obtained from the American Type Tissue Culture Collection, Rockville, MD, were grown in DMEM supplemented with heat inactivated 10% FBS, 20 mM HEPES, 100 U/ml penicillin, 100 μg/ml streptomycin, 1% L-glutamine and 1% sodium pyruvate. The cells were grown in a humidified atmosphere of 95% air/5% CO_2 at 37°C.

Cell transfection

Cells (150,000/well) were seeded into 6-well plates 24 hr prior to transfection in RPMI1640 antibiotics free (2 ml) and then transfected with 10 μg RSV-Raf-C4 or 10 μg RSV-Raf-BXB or 10 μg of empty vector (pRSV) by using Lipofectamine 2000 (LF2000) according to the manufacturer's instructions (Invitrogen, Carlsbad, CA). The plasmids were previously described.[26]

Drug combination studies

For the study of the synergism between IFNα and R115777 on cell growth inhibition of H1355 and KB, the cells were seeded in 96-multiwell plates at the density of 5×10^3 cells/well. After 24 hr incubation at 37°C, the cells were treated with different concentrations of R115777 and IFNα. Drug combination studies were based on concentration–effect curves generated as a plot of the fraction of unaffected (surviving) cells *versus* drug concentration after 72 hr of treatment. To explore the relative contribution of each agent to the synergism, 3 combinations with different R115777/ IFNα molar ratios were tested for each schedule: equiactive doses of the 2 agents (IC_{50}), higher relative doses of R115777 (IC_{75} of R115777/ IC_{25} of IFNα) and higher relative doses of IFNα (IC_{25} of R115777/IC_{75} of IFNα). Assessment of synergy was performed quantitating drug interaction by Calcusyn computer program (Biosoft, Ferguson, MO). Combination index (CI) values of <1, 1, and >1 indicate synergy, additivity and antagonism, respectively.[27] Furthermore, we analyzed the specific contribution of both R115777 and IFNα on the cytotoxic effect of the combination by calculating the potentiation factor (PF), defined as the ratio of the IC_{50} of either FTI or IFNα alone to the IC_{50} of FTI + IFNα combinations as described before; a higher PF indicates a greater cytotoxicity.[28]

Western blot analysis

KB cells were grown for 48 hr with or without IFNα and/or R115777 at 37°C. For cell extract preparation, the cells were washed twice with ice-cold PBS/BSA, scraped and centrifuged for 30 min at 4°C in 1 ml of lysis buffer (1% Triton, 0.5% sodium deoxycholate, 0.1 NaCl, 1 mM EDTA, pH 7.5, 10 mM Na_2HPO_4, pH 7.4, 10 mM PMSF, 25 mM benzamidin, 1 mM leupeptin, 0.025 U/ml aprotinin). Equal amounts of cell proteins were separated by SDS-PAGE. The proteins on the gels were electro-transferred to nitrocellulose and reacted with the different MAbs. For immunoprecipitations, anti-Bcl-2 MAb was added to cell lysates and incubated overnight at 4°C, and antibodies were collected on protein A Sepharose beads. Protein complexes were washed in an immunoprecipitation buffer (50 mM Tris-HCl, pH 7.4, 0.5 M NaCl, 1 mM $CaCl_2$, 1 mM $MgCl_2$, 0.1% Tween-20) before direct analysis by SDS-PAGE. The proteins were transferred on nitrocellulose film and reacted with anti-Raf-1 rabbit antiserum.

Affinity precipitation of Ras

KB cells were treated with IFNα and/or R115777 as described above. The cells were lysed in the Mg^{2+} buffer containing 20 mM HEPES, pH 7.5, 150 mM NaCl, 1% Igepal CA-630, 10 mM $MgCl_2$, 1 mM EDTA and 2% glycerol. Then, 10 μl Ras Binding Domain (RBD) conjugated to agarose (Cell Signaling Technology) were added to 1 mg of cell lysate and the resulting mixture was incubated o/n with gentle rocking at 4°C. The agarose beads were collected by microcentrifugation at 14,000*g* for 5 sec. and washed thrice with Mg^{2+} buffer. The agarose beads were boiled for 5 min in 2× Laemmli sample buffer and collected by a microcentrifuge pulse. The supernatants were run on 12% SDS-PAGE, then the proteins were electrotransferred on a nitrocellulose film. The nitrocellulose was incubated overnight with 1 μg/ml of anti-Ras Mab, clone RAS10 and with a secondary Mab, a goat α-mouse HRP conjugated IgG, for 1 hr. The film was washed with TBS/0.05% Tween 20 and detected by ECL, chemiluminescence's technique (Amersham).

The detection of the expression of active ras was performed as previously described.[17]

Confocal microscopy

KB cancer cells were seeded onto 35-mm culture dishes on sterile coverslips and allowed to attach for 24 hr. Subsequently, the cells were incubated for 10 min in the presence of IFNα and/or R115777 as described above. The medium was then removed, cells washed with PBS and fixed with 1 ml Cytofix/cytoperm (Pharmigen, CA, USA) for 45 min at 41°C. Subsequently, the fixation buffer was removed and cells washed with 1 ml of washing buffer. For visualization of bcl-2 and Raf-1, the cells were exposed to anti-bcl-2 MAb and anti-Raf-1 rabbit antiserum for 10 min at 41°C and washed with washing buffer. Subsequently the cells were exposed to both rhodamine–conjugated anti-mouse goat antiserum and FITC-conjugated anti-rabbit goat antiserum (DAKO, Bastrup, DK) for 10 min at 41°C. After final washes, coverslips were mounted on the dishes using a 50% solution of glycerol in PBS. For mitochondria visualization, the mitochondrial-selective dye, MitoTracker Green FM (Molecular Probes) was used. MitoTracker Green (1 μM) and anti-Raf-1 rabbit antiserum were added to each dish for 10 min at 37°C. Cells were washed twice in PBS. Subsequently, the cells were exposed to rhodamine–conjugated anti-rabbit goat antiserum for 10 min at 41°C. After final washes, the cells were examined under a LEICA TCS SP2 confocal microscope.

Flow cytometric analysis of apoptosis

Annexin V-FITC (fluorescein isothiocyanate) was used in conjunction with a vital dye, Propidium Iodide (PI), to distinguish apoptotic (Annexin V-FITC positive, PI negative) from necrotic (AnnexinV-FITC positive, PI positive) cells. Briefly, cells were incubated with Annexin-V–FITC (MedSystems Diagnostics, Vienna, Austria) and propidium iodide (Sigma, St. Louis, MO, USA) in a binding buffer (10 mM Hepes, pH 7.4, 150 mM NaCl, 5 mM KCl, 1 mM $MgCl_2$, 2.5 mM $CaCl_2$) for 10 min at room temperature, washed and resuspended in the same buffer. Analysis of apoptotic cells was performed by flow cytometry (FACScan, Becton Dickinson). For each sample, 2×10^4 events were acquired. Analysis was carried out by triplicate determination on at least 3 separate experiments.

AKT kinase assay

KB cells were treated with IFNα and/or R115777 as described above. At the time of processing 1 ml ice-cold Cell Lysis Buffer (20 mM TRIS, pH 7.5, 150 mM NaCl, 1 mM EDTA, 1 mM EGTA, 1% Triton X-100, 2.5 mM sodium pyrophosphate, 1 mM β-glycerophosphate, 1 mM sodium orthovanadate, 1 μg/ml leupeptine, 1 mM PMSF) was added to cells that were incubated on ice for 10 min. The cells were collected and transferred to microcentrifuge tubes and centrifuged at 1,200*g* for 10 min at 4°C. The supernatants were collected and precipitated with 20 μl of IgG1 anti-Akt monoclonal antibody immobilized with agarose beads (Cell Signaling Technology) by o/n incubation with gentle rocking at 4°C. The resulting immunoprecipitates were then incubated for 30 min at 30°C with 1 μg GSK-3 fusion protein (Cell Signaling Technology) in the presence of 200 μM ATP and Kinase Buffer (25 mM Tris, pH 7.5, 5 mM β-glycerophosphate, 2 mM dithiotreitol, 0.1 mM sodium orthovanadate, 10 mM $MgCl_2$). The reaction was terminated with the addition of 20 μl 3× SDS sample buffer. The supernatants were boiled for 5 min and electrophoresed by 12% SDS-PAGE and the protein electro-transferred on a nitrocellulose film. Phosphorylation of GSK-3 was detected using as probe an anti-Phospho-GSK-3α/β(Ser21/9) rabbit polyclonal antibody (diluted 1:1,000) and then with a secondary anti-rabbit HRP-conjugated monoclonal antibody, (diluted 1:2,000). The film was washed with TBS 1×-0.05% Tween 20 buffer and the specific reactivity was detected by chemiluminescence technique (Amersham) according to the manufacturer's instructions (Cell Signaling Technology).

In vivo *xenograft assay*

Female BALB/c athymic (nu^+/nu^+) mice, 8–10 weeks of age, 24–32 g body weight, were purchased from Charles River Laboratories (Milan, Italy). The research protocol was approved, and mice were housed and maintained under specific pathogen-free conditions in the animal care facility of National Cancer Institute Fondazione G. Pascale in agree with the institutional guidelines for Animal Care and Use Committee of the Italian ministry of health. Mice were acclimatized for 1 week prior to being injected with cancer cells. Mice were injected s.c. with 10^6 KB cells that had been resuspended in 200 μl of PBS. After 5 days, when established tumors of ~0.3 cm^3 in diameter were detected, mice were randomized and divided in to 4 groups. Ten mice/group were treated s.c. on Days 1, 3 and 5 of each week with 2×10^6 IU/kg/dose IFNα diluted in PBS and/or 20 mg/kg/dose R115777 p.o. twice a day diluted in polyethylene glycole (PEG) 400, for 3 weeks.[1,29] Control animals received equal volume of PEG p.o. in the same way of animals receiving R115777 and were injected with equal volume of PBS as animals receiving IFNα. Tumor size was measured twice weekly by the modified ellipsoid formula $\pi/6$ *AB*, where *A* is the longest and *B* the shortest perpendicular axis of an assumed ellipsoid corresponding to tumor mass.[30] Body weight was measured twice a week as control for treatment toxicity. Two-sided Student's *t* test was used to compare the volume of xenograft tumors. For the calculation of CI, the values of % of cell kill for a fixed tumor volume (determined by the log cell kill) were considered. Log cell kill (LCK) was determined as $LCK = (T - C)/3.32 \times T_d$, where T_d represents the mean doubling time of control group required to reach a fixed tumor volume, expressed in days, while *T* and *C* are the mean times in days required to reach the same fixed tumor volume in the treated groups and control group, respectively. Cell Kill (CK) was determined as $\%\ CK = [1 - (1 - 10^{LCK})] \times 100$.[31]

Tumor growth delay (TGD) was determined as $\%TGD = [(T - C)/C] \times 100$, where *T* and *C* are the same values as described above.[31] Log cell kill (LCK) and tumor growth delay (TGD) was determined as previously described.[31]

Immunohistochemistry

Briefly, sections from each specimen were cut at 3–5 μm, mounted on glass and dried overnight at 37°C. All sections then were de-paraffinized in xylene, rehydrated through a graded alcohol series and washed in PBS. This buffer was used for all subsequent washes and for dilution of the antibodies. Tissue sections were heated twice in a microwave oven for 5 min each at 700 W in citrate buffer (pH 6) and then processed with the standard streptavidin-biotin-immunoperoxidase method (DAKO Universal Kit, DAKO Corporation, Carpinteria, CA). Rabbit polyclonal immune serum raised against EGF-R, phospho-EGF-R (Cell Signaling) at a 1:50 dilution, rabbit polyclonal immune serum raised against Erk and pErk (Cell Signaling) at a 1:100 dilution (Cell Signaling Technology), were the primary antibodies incubated for 1 hr at room temperature.

Diaminobenzidine was used as the final chromogen, and hematoxylin as the nuclear counterstain. Negative controls for each tissue section were performed leaving out the primary antibody. The specificity of staining was also confirmed by competition of the primary antibodies with the respective peptide to which they were generated (data not shown). All samples were processed under the same conditions. Two pathologists evaluated the staining pattern of the two proteins separately and scored the protein expression in each specimen for the percentage of positive neoplastic cells: score 0, undetectable staining; score 1, from 1 to 30% of positive cells; score 2, from 30 to 60% of positive cells; score 3, more than 60% of positive cells. Analysis of the data using such necessarily arbitrary cut-offs was highly statistically significant and, therefore, functionally operative. A total of 500 cells was counted in each specimen. All samples were processed as previously described.[17]

In vivo *apoptosis detection*

Apoptotic cells were identified by using the peroxidase-based Apoptag kit (Oncor, Gaitherburg, MD) method. Dewaxed and rehydrated specimens were incubated in proteinase K 40 μg/ml for 1 hr at 37°C and were treated with 3% H_2O_2 in methanol for 30 min at room temperature. After adding equilibration buffer for 5 min at room temperature, terminal deoxynucleotidyl transferase (TdT) enzyme was pipetted onto the sections and incubated at 37°C for 2 hr. The reaction was stopped by incubating the sections in stop buffer for 30 min at 37°C. Antidigoxigenin peroxidase was added to the slides, followed by incubation for 30 min at 37°C. Slides were stained with diaminobenzine for 10 min and counterstained with hematoxylin. A total of 500 cells was counted in each specimen. The Apoptotic Index was defined as follows: Apoptotic Index (%) = 100 × apoptotic cells/total cells.

Statistical analysis

All data are expressed as mean + SD. Statistical analysis was performed by analysis of variance (ANOVA) with Neumann-Keul's multiple comparison test or Kolmogorov-Smirnov where appropriate. The statistical analysis of Kaplan-Meyer plots was performed with Log-Rank Test (MedCalc).

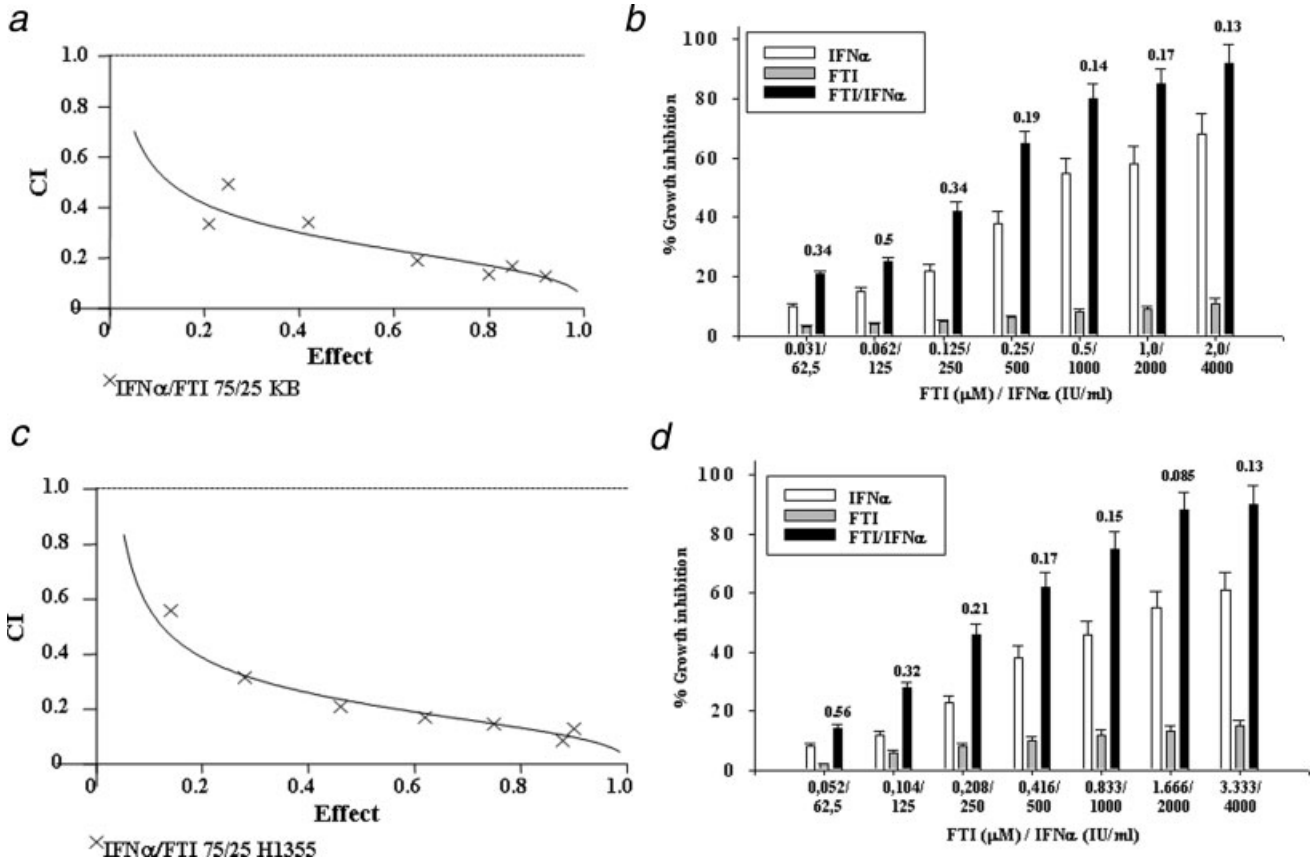

Figure 1 – IFNα and the FTI R115777 have a synergistic effect on KB cell growth inhibition. We have evaluated the growth inhibition induced by different concentrations of IFNα and R115777 at 72 hr on KB and H1355 cells. We have performed these experiments with MTT assay and the resulting data were elaborated with the dedicated software Calcusyn (by Chou and Talalay) as described in "Material and methods". CI/effect curves showed the CI *versus* the fraction of cells affected/killed by R115777 and IFNα in combination for the KB (*a*) and H1355 (*c*) cell lines when higher relative doses of IFNα(IC_{25} of R115777/IC_{75} of IFNα) were used. Combinations were synergistic when CIs were <1. Representative values of growth inhibition induced by R115777 and IFNα alone or in combination at different concentrations are reported for KB (*b*) and H1355 (*d*) cells. The CIs values for each combination are showed in the graph on the columns representing the different combination values. Bars, SEs. Each point is the mean of at least 4 different replicates. ☐ IFNα: IFNα-treated cells; ■ FTI: R115777-treated cells; ▒ FTI/IFNα: IFNα + R115777-treated cells.

Results

IFNα and the FTI R115777 synergize on KB and H1355 cell growth inhibition

IFNα concentrations, which are capable of producing growth inhibitory and pro-apoptotic effects on solid tumor cells *in vitro*, are difficult to reach *in vivo*. We have recently demonstrated that IFNα induces an EGF-Ras→Erk-dependent antiapoptotic signaling in human epidermoid cancer cells.[17] Based upon these results, we have investigated whether the Ras inhibitor FTI R115777 could have synergistic effects on cell growth inhibition in combination with IFNα. Therefore, we have evaluated the growth inhibition induced by different concentrations of R115777 in combination with IFNα at 72 hr on KB and H1355 cells. We have performed these experiments with MTT assay and the resulting data were elaborated with the dedicated software Calcusyn (by Chou and Talalay, see also "Material and methods"). With this mathematical model, synergistic conditions occur when the combination index (CI) is below 1.0. When CI is less than 0.5 the combination is highly synergistic. We have found that the combination of IFNα and R115777 was highly synergistic when the 2 drugs were used at either ratios with higher concentrations of IFNα or equitoxic ratios on both KB (Fig. 1*a* and data not shown, respectively) and H1355 (Fig. 1*c* and data not shown, respectively) cell lines. On the other hand, antagonism was recorded when ratios with higher concentrations of R115777 were used (Table I). In synergistic drug combination the CI_{50s} (the combination index calculated for 50% cell survival by isobologram analysis) were, at equitoxic ratios and ratios with higher concentrations of IFNα, respectively, 0.66 and 0.27 for KB and 0.75 and 0.22 for H1355 cells (Table I). The synergism between the 2 agents in these experimental conditions is also demonstrated by the representation of the growth inhibition values for the different combinations used for the calculation of CIs (Figs. 1*b* and 1*d*). In fact, in the different combinations the sum of the growth inhibition induced by the single agents was always less than the growth inhibition caused by the combination. Therefore, the combined use of the 2 agents was highly synergistic on the growth inhibition of both cell lines. Dose reduction $index_{50}$ (DRI_{50}) represents the magnitude of dose reduction obtained for the 50% growth inhibitory effect in combination setting when compared to each drug alone. In our experimental conditions, the DRI_{50} of IFNα and R115777 were equal to 3.7 and 2.6 in KB and 1.8 and 4.9 in H1355 cells, respectively, when the 2 drugs were used at equitoxic ratios (Table I). Moreover, the DRI_{50} of IFNα and R115777 were equal to 3.9 and 135.6 in KB and 4.6 and 246.1 in H1355 cells, respectively, when IFNα was used at ratios with higher concentrations (Table I). Moreover, values of PF reported

TABLE I – DOSE REDUCTION INDEX (DRI),[1] COMBINATION INDEX (CI)[2] VALUES ACCORDING TO THE DIFFERENT CYTOTOXIC RATIO OF IFNα/R115777 COMBINATION AND POTENTIATION FACTOR (PF)[3] VALUES OF IFNα AND R115777

Cell lines	50:50 Cytotoxic ratio				25:75 Cytotoxic ratio				75:25 Cytotoxic ratio			
	IFNα/R115777				IFNα/R115777				IFNα/R115777			
	DRI_{50} (± SD)	CI_{50} (± SD)	PF IFNα (± SD)	PF R115777 (± SD)	DRI_{50} (± SD)	CI_{50} (± SD)	PF IFNα (± SD)	PF R115777 (± SD)	DRI_{50} (± SD)	CI_{50} (± SD)	PF IFNα (± SD)	PF R115777 (± SD)
KB	3.675 (0.438)	0.662 (0.188)	2.5 (0.253)	2.5 (0.22)	6.326 (0.63)	1.06 (0.45)	4.3 (0.38)	1.1 (0.11)	3.885 (0.4)	0.265 (0.036)	2.7 (0.23)	133.3 (14.5)
	2.565 (0.241)				1.104 (0.11)				135.58 (13.6)			
H1355	1.818 (0.18)	0.755 (0.11)	1.8 (0.178)	1.8 (0.16)	4.921 (0.5)	1.12 (0.24)	4.9 (0.53)	0.4 (0.056)	4.586 (0.46)	0.222 (0.036)	4.5 (0.48)	92.6 (9.23)
	4.878 (0.532)				1.1 (0.11)				246.146 (23.8)			

[1]DRI values (mean ± standard deviation from at least 3 separate experiments performed in quadruplicates) represent the order of magnitude (fold) of dose reduction obtained for IC_{50} (DRI_{50}) in combination setting compared with each drug alone. 50:50 cytotoxic ratio, equipotent doses of the two agents [IFNα (IC_{50})/R115777(IC_{50})]; 25:75 cytotoxic, evaluation of CIs at higher relative doses of R115777 [IFNα (IC_{25})/R115777(IC_{75})]; 75:25 cytotoxic, evaluation of CIs at higher relative doses of IFNα [IFNα(IC_{75})/R115777(IC_{25})].–[2]CI values (mean ± standard deviation from at least 3 separate experiments performed in quadruplicates) represent the assessment of synergy induced by drug interaction. Combination index (CI) values of <1, 1 and >1 indicate synergy, additivity and antagonism, respectively.–[3]PF values (mean ± standard deviation from at least 3 separate experiments performed in quadruplicates) defined the specific contribute of IFNα or R115777 evaluated as the ratio of the IC_{50} of IFNα or R115777 to the IC_{50} of IFNα/R115777. The Friedman nonparametric rank test was used to analyze the impact of the different cytotoxic ratio on the whole cell line panel, $p = 0.018$.

in Table I demonstrated that R115777 had an important contribution to the cytotoxic effect of the combination in both cells. Interestingly, the optimal results (lowest CI values with the best PF) were obtained when higher concentrations of IFNα were used (75:25 concentrations ratio) (Table I). These results demonstrate that a strong or a very strong synergism can be recorded on cell proliferation when the 2 drugs are used in combination. Effective concentrations in the combinatory experiments are possible to be reached *in vivo*.

IFNα and the FTI R115777 synergize on apoptosis induction in epidermoid cancer cells

We have selected 2 concentrations of R115777 and IFNα that were highly synergistic at Calcusyn elaboration and we have evaluated the apoptotic effects of their combination with FACS analysis after labeling for annexin V. We have used this combination also for all subsequent experiments on the perturbation of intracellular signaling. We have found that the treatment with 0.07 μM R115777 and 500 IU/ml IFNα alone for 48 hr induced apoptosis in only 16–19% of cell population *versus* 5% of untreated cells as demonstrated with FACS analysis (Fig. 2*a*–2*c* and 2*f*). However, when the cells were treated with the 2 drugs in combination for 48 hr 49% of apoptosis was found (Figs. 2*d* and 2*f*). The addition of 50 μM VP-16 for 48 hr was used as positive control and induced about 53% of apoptosis (Figs. 2*e* and 2*f*).

Similar results were obtained on H1355 cells. In fact, the 2 agents alone induced about 20 and 25% apoptosis at 48 and 72 hr of treatment, respectively, while the combination caused apoptosis in about 60 and 80% of cell population at 48 and 72 hr, respectively (Fig. 2*g*). Since it has been reported that FTIs can induce apoptosis in tumor cells through the induction of the expression of the death domain receptor Fas we have investigated whether the synergistic effects on apoptosis induced by the combination between R115777 and IFNα were paralleled by an increase of Fas expression.[32] However, we have found that the synergistic effects of the combination are likely independent from the induction of Fas surface expression in these 2 cell lines (data not shown).

These data suggest that the synergism on cell growth inhibition induced by IFNα and R115777 could be mediated by the induction of apoptosis in human epidermoid cancer cells.

IFNα and R115777 combination antagonizes activation of Ras-dependent survival pathways

We have evaluated both the expression and activity of Ras in the different treatment settings. We have found that the single agents and the combination as well as 10 nM EGF for 10 min did not affect the expression of Ras (Fig. 3*a*). However, R115777 used at low concentrations (0.07 μM) for 48 hr caused only about 0.2-fold decrease of the Ras activation ratio (calculated as the ratio between the intensities of the bands associated with ras activity and expression, respectively). On the other hand, 500 IU/ml IFNα induced an about 3-fold increase of the activity of the protein similarly to EGF (about 3.5-fold) (Figs. 3*a* and 3*b*). However, R115777 completely antagonized the effect of IFNα, thus restoring Ras activity to the levels of low dose R155777-treated cells (Figs. 3*a* and 3*b*).

Thereafter, we have evaluated the effects of IFNα and R115777 on the terminal enzymes of the survival MAPK pathway, Erk-1 and Erk-2. The addition of EGF induced again about 3.5-fold increase of Erk-1 and 2 activity without changing their expression (Figs. 3*d* and 3*c*, respectively). On the other hand, we have found that 48 hr 0.07 μM R115777 induced about 0.2-fold reduction of Erk-1/2 activity while IFNα alone caused about 3-fold increase (Figs. 3*d* and 3*h*). The combined treatment restored Erk-1/2 activity to that one of R115777-treated cells (Figs. 3*d* and 3*h*). All the treatments had no effects on the expression of these enzymes, thus suggesting a direct effect on enzyme activation induced by the upstream regulators more than on enzyme expression/content (Fig. 3*c*). Thereafter, we have evaluated the

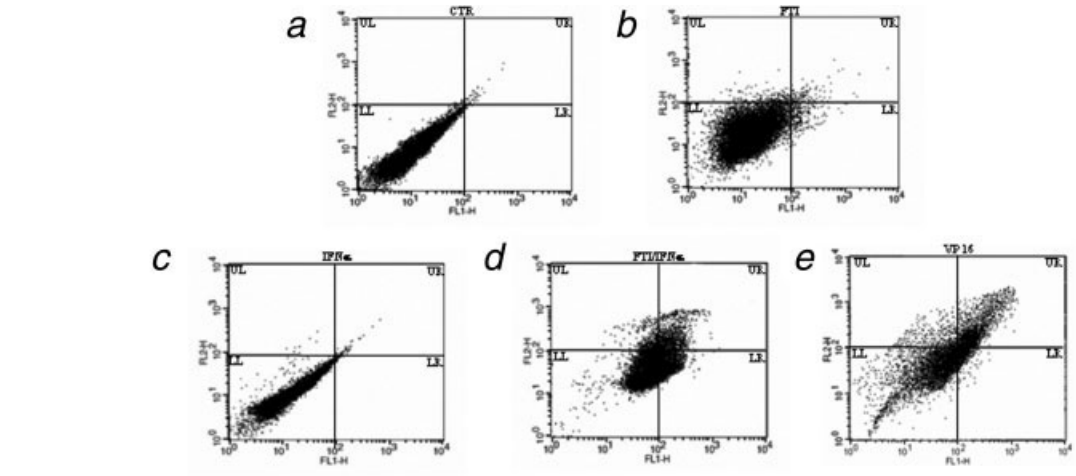

f

Quad	% Total				
	CTR	FTI	IFNα	FTI/IFNα	VP 16
UL	1.65	4.82	2.55	7.92	7.86
UR	2.15	8.14	5.86	17.59	23.83
LL	94.91	70.75	83.97	50.85	47.37
LR	1.29	9.29	7.52	23.64	20.94

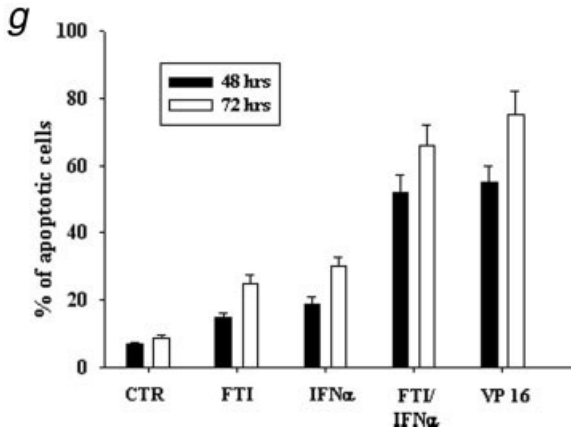

Figure 2 – Apoptotic effects of IFNα and R115777 combination on human epidermoid KB and H13555 cells. (*a–e*) FACS analysis PI/Annexin V labeling of KB cells treated with 0.07 μM R115777 and/or 500 IU/ml R115777 for 48 hr. (*a*) Untreated cells; (*b*) 48 hr 0.07 μM R115777; (*c*) 48 hr 500 IU/ml IFNα; (*d*) 48 hr 500 IU/ml IFNα + 0.07 μM R115777; (*e*) 48 hr 50 μM VP16. The experiments were performed at least thrice and the results were always similar. Bars, % of apoptotic cells. (*f*) Percentage of cells for each quadrant. Lower left (LL) are both Annexin V-FITC and PI negative; upper left (UL) are PI positive indicating necrosis; lower right (LR) are Annexin V-FITC positive indicating early apoptosis; upper right (UR) are both Annexin V-FITC and PI positive indicating late apoptosis. (*g*) The percent of apoptotic cells evaluated by FACS analysis after Annexin V labeling of H1355 cells treated with 0.07 μM R115777 and/or 500 IU/ml R115777 for 48 hr (white columns) or 72 hr (black columns). Bars, SEs. The experiments were performed at least thrice and the changes were statistically significant. CTR, untreated; FTI, 0.07 μM R115777; IFNα, 500 IU/ml IFNα; IFNα + FTI, 500 IU/ml IFNα + 0.07 μM R115777; VP16, 50 μM VP16.

effects of these agents on another important survival pathway regulated by Ras, the Akt/PKB signaling. We have found that 48 hr 0.07 μM R115777 induced about 0.25-fold reduction of Akt activity while IFNα alone caused about 3-fold increase of Akt activity without apparent modifications of its expression (Figs. 3*e*, 3*f* and 3*h*). The addition of 10 nM EGF for 10 min induced again a 3.5-fold increase of Akt activity. The concomitant treatment again restored Akt activity to that one of R115777-treated (Fig. 3*e*).

All these data demonstrate that the synergistic effects of IFNα/R115777 combination on growth inhibition and apoptosis in epidermoid cancer cells are paralleled by the downregulation of Erk and Akt activity, indicating the suppression of survival pathways induced by IFNα and mediated by Ras in these cells.

In vivo *cooperative antitumor effect of IFNα in combination with R115777*

To examine the *in vivo* interaction between R115777 and IFNα and to evaluate the potential therapeutic effects of the combination, athymic mice were s.c inoculated with KB cells. The KB s.c. tumors were allowed to grow until approximately 0.2–0.3 cm^3 before randomization in four groups: control, R115777, IFNα and R115777 plus IFNα.

On the basis of pilot studies (data not shown), doses of both agents were specifically selected so that their independent effects on tumor growth inhibition would be modest. Mice were administered with R115777 at the dose of 20 mg/kg p.o. twice daily for 3 weeks and/or IFNα at the dose of 50,000 IU s.c., thrice a week for 3 weeks. The administration modalities of the 2 drugs were similar to those reported in humans and appear to be relevant to clinical situation.[1,29,33] Tumor growth was evaluated thrice a week and both mean tumor volume (Fig. 4*a*) and tumor growth delay were calculated (Fig. 4*b*).

As shown in Figure 4*a*, 21 days after the beginning of treatment in mice treated with IFNα alone, the mean tumor volume was only 5% decreased when compared to untreated mice and 4% tumor growth delay was observed (Figs. 4*a* and 4*b*, respectively). The treatment with R115777 alone produced 8% tumor volume reduction and tumor growth delay when compared to untreated mice (Figs. 4*a* and 4*b*, respectively). These differences were not statistically significant ($p > 0.05$). On the other hand, the mean tumor volume in mice treated with the R115777/IFNα combination was about 35% reduced if compared with control groups ($p = 0.002$, Fig. 4*a*). In the same group, an about 40% tumor growth delay was also recorded (Fig. 4*b*). Furthermore, the *in vivo* synergistic effect between IFNα and R115777 described above was

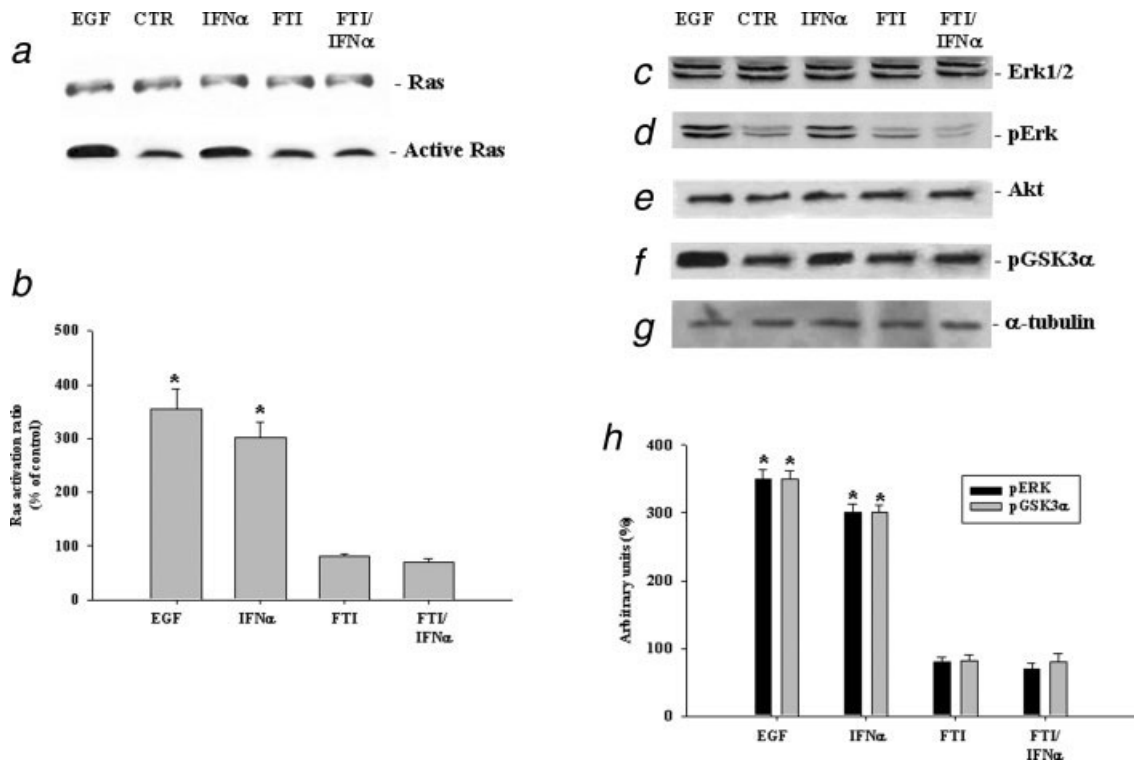

Figure 3 – Effects of IFNα and R115777 on Ras, Erk and Akt expression and activity. (*a*) Western blot assay for the expression of the total Ras protein (upper gel). Affinity precipitation of Ras performed with the minimal binding domain of Raf-1 conjugated with agarose for the evaluation of Ras activity as described in "Material and methods" (lower gel). CTR, untreated; EGF, 10 min 10 nM EGF; IFNα, 48 hr 500 IU/ml IFNα; FTI, 48 hr 0.07 μM R115777; IFNα + FTI, 48 hr 500 IU/ml IFNα + 0.07 μM R115777. (*b*) Representation of the Ras activation ratio expressed as the ratio between the relative intensities of the bands associated with activated Ras *versus* the bands associated with total Ras. The evaluation was performed with the dedicated software after laser scanner and computer-assisted acquisition of the bands. The intensity of each band was calculated in relative intensity when compared to that of the untreated cells. The cells were also processed for the determination of the expression (*c*) and phosphorylation (*d*) of Erk-1 and 2 evaluated after blotting with an anti-MAPK and an anti-pMAPK specific Mab, respectively, as described in "Material and methods". In the same experimental conditions the expression (*e*) and activity (*f*) of Akt was also analyzed with a western blotting and a kinase assay using GSK3 as specific substrate of Akt, respectively, as described in "Material and methods". (*g*) Expression of the house-keeping protein α-tubulin, used as loading control. (*h*) Laser scanner of the bands associated to pErk and Akt activity. The intensities of the bands were expressed as % arbitrary units. Bars, SEs. The experiments were performed at least 3 different times and the results were always similar. CTR, untreated; EGF, 10 min 10 nM EGF; IFNα, 48 hr 500 IU/ml IFNα; FTI, 48 hr 0.07 μM R115777; IFNα + FTI, 48 hr 500 IU/ml IFNα + 0.07 μM R115777. Asterisks indicate the statistical significance of the data ($p < 0.005$).

also confirmed by the evaluation of combination index values evaluated as CI/ % of cell kill by Calcusyn software as described in "Material and methods" section (Fig. 4*c*). In fact, the CI_{50} was 0.2 and the DRI_{50s} were 11 and 9 for IFNα and R115777, respectively (Fig. 4*c*).

Combinatory treatment of R115777 plus IFNα was well tolerated, as demonstrated by maintenance of body weight (data not shown) and by the absence of other signs of acute or delayed toxicity. The cooperative effect of the combination on tumor growth *in vivo* was confirmed by the analysis of animal survival. In fact, the median survival time of both control and IFNα groups was 58 days while that of R115777 group was 62 days and of IFNα/ R155777 group 68 days (Fig. 4*d*). All mice died within 66, 66 and 68 days after tumor cell injection in the control, IFNα and R115777 groups, respectively (Fig. 4*d*). In contrast, 6 out of 10 mice treated with the combination of R115777 and IFNα were still alive after 78 days from the beginning of treatment when they were killed ($p = 0.042$; Fig. 6*d*).

The apoptotic rate of tumor tissues collected from mice was determined with TUNEL assay. The *in vivo* data confirmed the results obtained *in vitro*, suggesting an increase of the apoptotic index in tumor tissues collected from mice treated with the combination between R115777 and IFNα (Table II). In fact, the apoptotic rate was 0.25–1% in control group and 4–5% and 3–5% in IFNα and R115777-treated groups, respectively, while in the group treated with the combination 13–15% apoptosis was recorded (Table II, $p > 0.05$). A representative example of TUNEL staining in tumor tissues is shown in Figure 5*a*. These results suggest that a cooperative effect of the combination could be recorded also *in vivo*.

Finally, we evaluated whether the effect of R115777 and IFNα on EGF-R, and Erks expression and activation observed *in vitro* could be also obtained *in vivo*. As shown in Table II both EGF-R expression and phosphorylation were increased in IFNα-treated tumors and unchanged ($p > 0.05$) in R115777-treated cancers. In these experimental conditions, R115777 was not able to antagonize the EGF-R over-activation induced by IFNα. Moreover, we have evaluated the effects on Ras expression and activity and we have performed the laser scanner of the bands associated to total and activated Ras, thus calculating the Ras activation ratio (RasAR). We have found that IFNα alone caused an about 40% mean increase of RasAR ($p = 0.02$) while R115777 alone induced no significant changes of RasAR ($p > 0.05$) (Figs. 5*b*–5*d*). However, when cells were treated with the 2 agents an about 40% mean decrease of RasAR was recorded ($p = 0.03$) (Figs. 5*b*–5*d*). The activity of Erk, the enzyme downstream to Ras, was increased in IFNα-treated xenografts ($p = 0.04$), unchanged in FTI-treated group and significantly decreased ($p < 0.05$) in xenografts of combination group (Table II). Erk expression was almost unchanged by the different treatments with the exception of a slight, but statis-

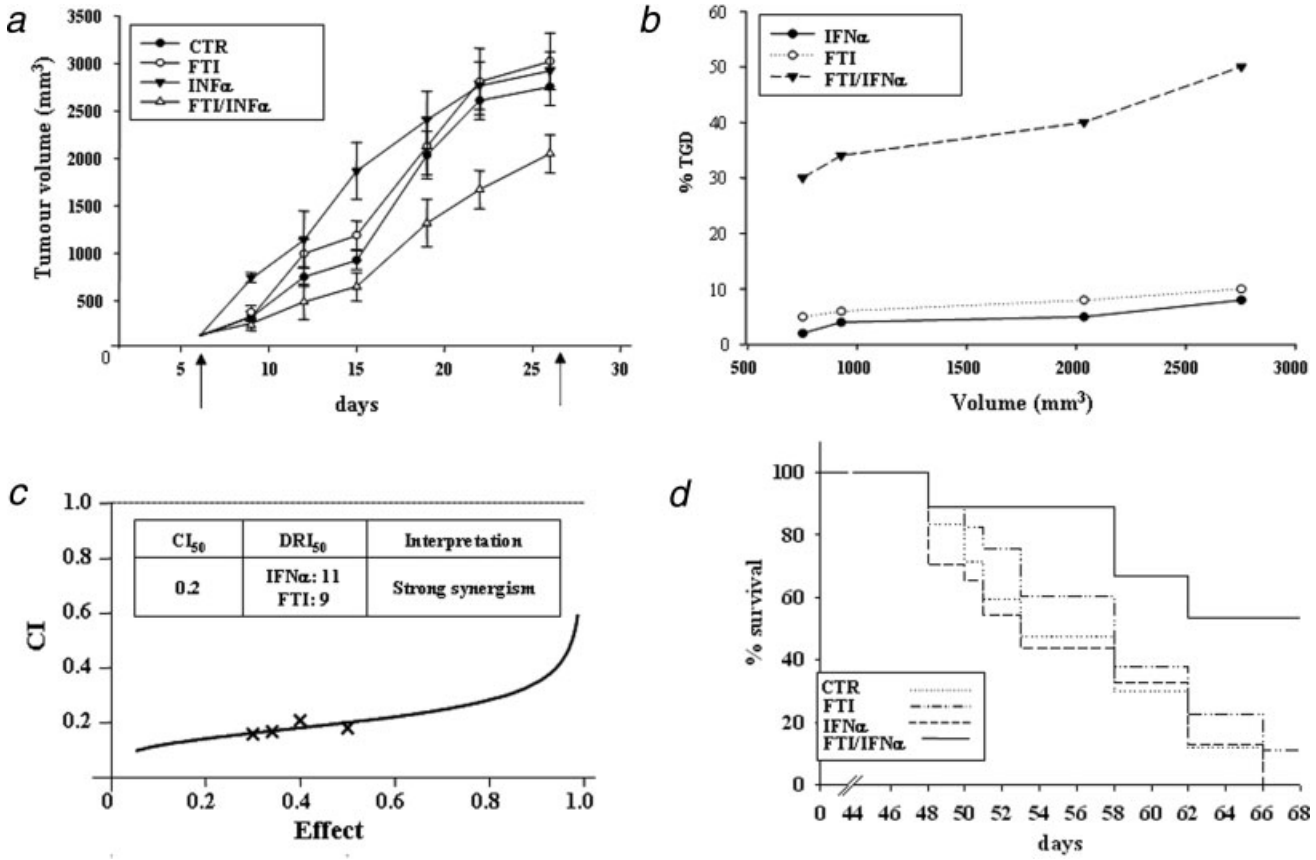

FIGURE 4 – Antitumor activity of R115777 and IFNα on established HNSCC KB xenografts. (*a*) Growth inhibition of KB xenografts in nude mice. KB cells (5×10^6) were s.c. injected in athymic mice as described in "Material and methods". After 6 days (average tumor size, 0.2–0.3 cm^3), mice were treated with R115777 on Days 1 to 6 of each week for 3 weeks and 3 days weekly with s.c. IFNα or with both drugs. Points, average tumor volume measured in each mouse of the group. Bars, SEs. Student's *t* test was used to compare tumor size among different treatment groups. Asterisks indicate the statistical significance of the data ($p < 0.005$). ● CTR: untreated cells; ○ FTI: R115777-treated cells; ▼ IFNα: IFNα-treated cells; △ FTI/IFNα: IFNα + R115777-treated cells. (*b*) effect of IFNα and/or R115777 on TGD. TGD was determined as %TGD $= [(T - C)/C] \times 100$, where *T* and *C* are the mean times expressed in days for the treated or control groups, respectively, to reach a defined tumor volume as described in "Material and methods". ● IFNα: IFNα-treated cells; ○ FTI: R115777-treated cells; ▼ FTI/IFNα: IFNα + R115777-treated cells. (*c*) *In vivo* IFNα + R115777 combination studies evaluated by CalcuSyn. For the calculation of CI, the values of % CK for a fixed tumor volume were considered. LCK was determined as LCK $= (T - C)/(3.32 \times T_d)$, where T_d represents the control group tumor volume doubling time, expressed in days, whereas *T* and *C* are the same as described above. CK was determined as % CK $= [1 - (1 - 10^{LCK})] \times 100$ as described in "Material and methods". In the insert the different CI_{50} and DRI_{50} values derived from the previous experiment are reported. (*d*) Analysis of the survival of the different groups of animals treated with the different combinations shown as Kaplan-Meyer plot. ····· CTR: untreated cells; -·-·- FTI: R115777-treated cells; ---- IFNα: IFNα-treated cells; —— FTI/IFNα: IFNα + R115777-treated cells. Asterisks indicate the statistical significance of the data ($p < 0.005$).

TABLE II – IMMUNOHISTOCHEMICAL ANALYSIS OF TUMOURS COLLECTED FROM MICE AFTER 4 WEEKS OF TREATMENT

Mouse No.	TUNEL *(% positive cells)*	EGF-R*	pEGF-R*	P-Erk-1/2*	Erk-1/2*	
1	0.25	1	1	1	2	CTR
2	1	2	1	2	2	CTR
7	0.25	2	1	3	2	CTR
9	4	3	3	3	3	IFNα
12	5	3	3	3	3	IFNα
15	4	3	3	2	2	IFNα
19	5	2	2	2	2	FTI
20	3	2	1	2	3	FTI
22	4	2	1	2	3	FTI
26	15	2	2	1	3	IFNα+FTI
28	14	3	3	1	3	IFNα+FTI
29	13	3	3	0	3	IFNα+FTI

*Score 0, undetectable staining; score 1, from 1 to 30% of positive cells; score 2, from 30 to 60% of positive cells; score 3, more than 60% of positive cells.

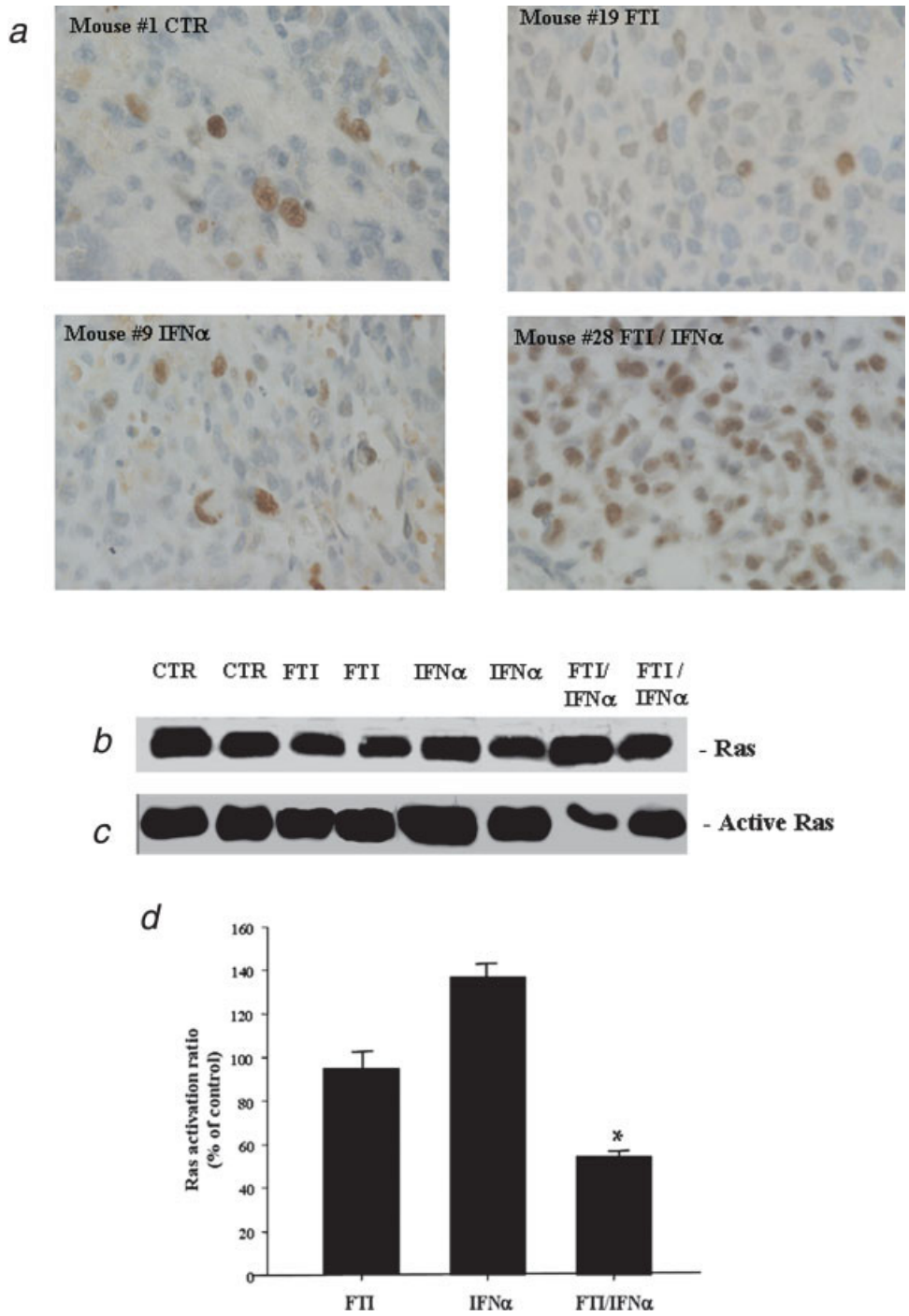

Figure 5 – Apoptosis and Ras activity evaluation in tumor xenografts collected from mice. (*a*) Representative images of TUNEL staining on human tumor KB cell xenografts collected from nude mice. Positive cells in brown are shown. CTR, untreated; IFNα, IFNα-treated; FTI, R115777-treated; IFNα + FTI, IFNα + R115777-treated. (*b*) Western blot assay for the expression of the total Ras protein. (*c*) Affinity precipitation of Ras performed with the minimal binding domain of Raf-1 conjugated with agarose for the evaluation of Ras activity as described in "Material and methods". CTR, untreated; IFN, IFNα-treated; FTI, R115777-treated; IFN + FTI, IFNα + R115777-treated. The experiments were performed at least 3 different times and the results were always comparable. (*d*) Representation of the Ras activation ratio expressed as the ratio between the relative intensities of the bands associated with activated Ras *versus* the bands associated with total Ras. The evaluation was performed with the dedicated software after laser scanner and computer-assisted acquisition of the bands. The intensity of each band was calculated in relative intensity as compared to that one of the untreated cells. Bars, SEs. Asterisks indicate the statistical significance of data ($p < 0.005$).

tically significant ($p < 0.05$) increase in xenografts treated with the combination (Table II). These data suggest that IFNα increased the EGF-Ras-Erk-dependent pathway also *in vivo* and that R115777 antagonized this pathway through the inactivation of ras.

IFNα/R115777 combination antagonizes the IFNα-induced translocation of Raf-1 to mitochondria

Since it has recently been described that Raf-1, once activated, can translocate to the mitochondria where it displaces bcl-2 from bad we

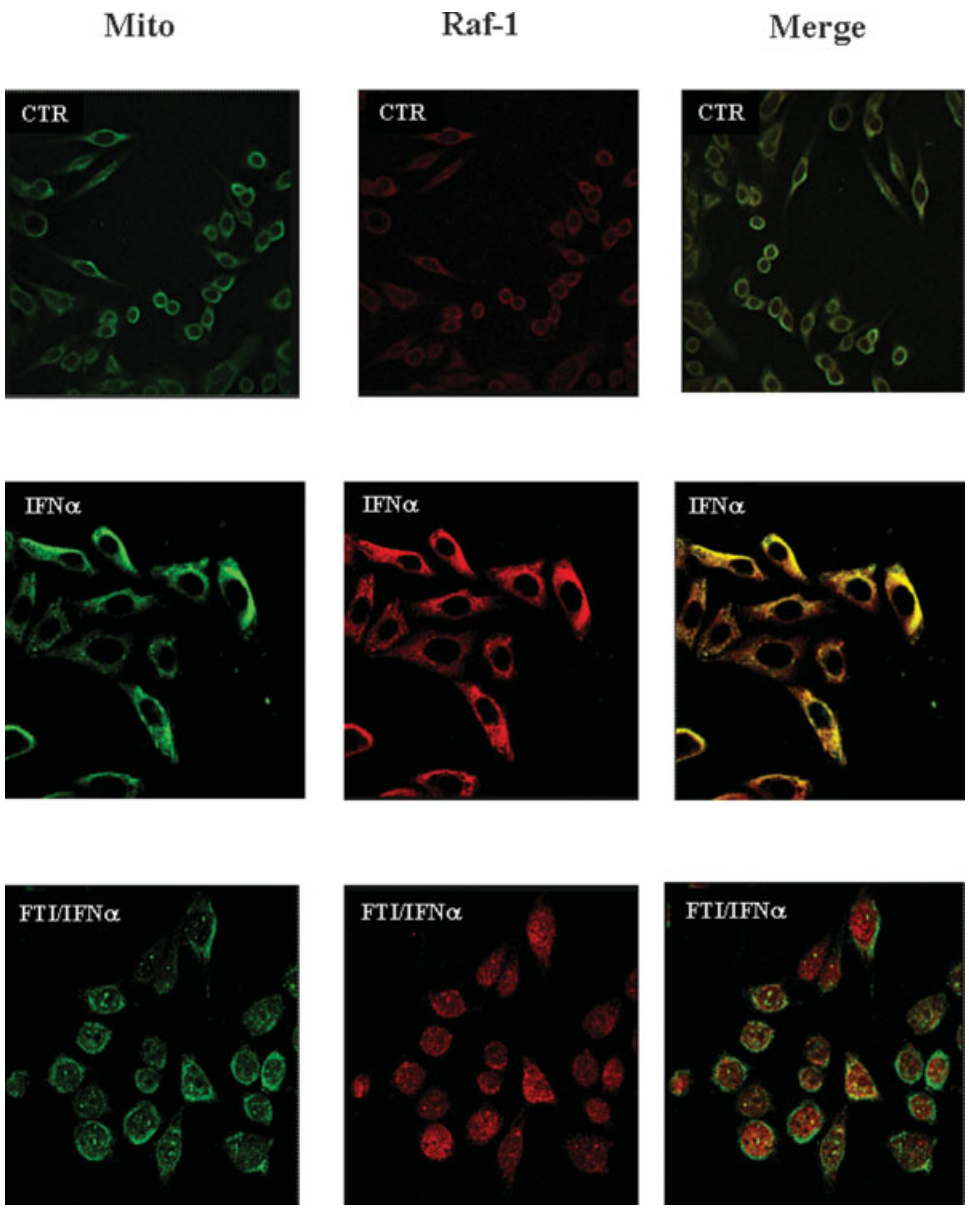

FIGURE 6 – Localization of Raf-1 in mitochondria in KB cells. KB cells were treated with 500 IU/ml IFNα and/or 0.07 μM R115777 for 48 hr and processed for the visualization of mitochondria and Raf-1 at confocal microscopy as described in "Material and methods". Mito: mitochondria visualization; Raf-1: Raf-1 immuno-visualization; Merge: fluorescence overlapping. CTR, untreated; FTI, 48 hr 0.07 μM R115777; IFNα, 48 hr 500 IU/ml IFNα; IFNα + FTI, 48 hr 500 IU/ml IFNα + 0.07 μM R115777. The experiments were performed at least 3 different times and the results were always comparable.

have evaluated the mitochondrial localization of Raf-1 with confocal microscopy.[34] We have found that Raf-1 is partially localized in mitochondria in untreated cells (Figs. 6*a*–6*c*) and the co-localization is strongly increased in IFNα-treated KB cells (Figs. 6*d*–*6f*). However, the treatment of KB cells with the combination completely antagonized this effect (Figs. 6*g*–*6i*). These data confirmed that, following its activation induced by IFNα treatment, Raf-1 is translocated to the mitochondria where it likely interacts with bcl-2 increasing the antiapoptotic properties of the latter. R115777 antagonizes these effects through the inhibition of Ras, the upstream activator of Raf-1.

IFNα/R115777 combination antagonizes the molecular interaction/co-localization of Raf-1 with bcl-2 and the consequent BAD phopshorylation in ser112

Raf-1, the immediately downstream target of Ras, has been reported to activate bcl-2 through interaction and subsequent phosphorylation on serine-70 of bcl-2 and displacement of bcl-2 from bad.[34] To determine the molecular mechanisms at the basis of the survival function of the Ras→Raf-1-dependent pathway in IFNα-treated cells, we have transfected KB cells with either dominant negative (DN) RSV-Raf-C4 or dominant positive (DP) RSV-Raf-BXB. Thereafter, we have examined both the activation of Erk-dependent pathway and the molecular interaction between Raf-1 and bcl-2. The transfection with DN Raf-1 induced a reduction of Erk activity (30% of control) that was partially restored by IFNα (78% of control) and slightly decreased by R115777 (10% of control) (Figs. 7*a* and 7*g*). The combination was again able to antagonize the over-activation of Erks induced by IFNα (20% of control) (Figs. 7*a* and 7*g*). On the other hand, the transfection of KB cells with the DP Raf-1 caused a significant increase of Erk activity (180% of control) that was not modulated by IFNα (178% of control) since the pathway was already hyperactivated by the transfec-

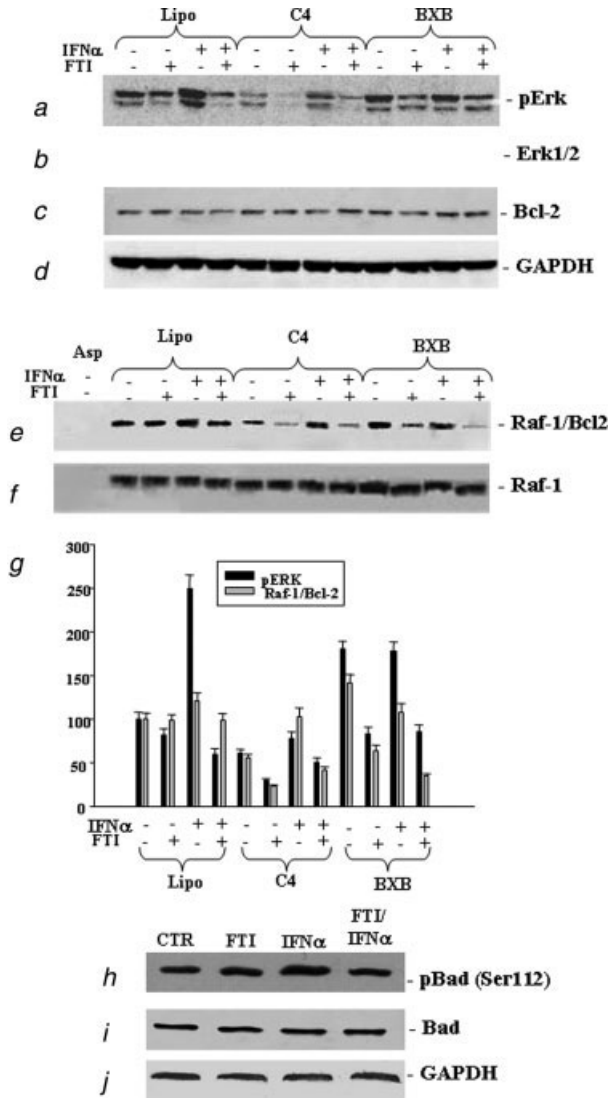

Figure 7 – Study of Bcl-2/Raf-1 interaction and Bad phosphorylation. KB cells were lipo-transfected with either dominant negative (DN) RSV-Raf-C4 or dominant positive (DP) RSV-Raf-BXB treated with 500 IU/ml IFNα and/or 0.07 μM for 48 hr and processed for the determination of the phosphorylation (*a*) and expression (*b*) of Erk-1/2 evaluated after blotting with anti-pMAPK and anti-MAPK specific Mabs, respectively, as described in "Material and methods". (*c*) Expression of the house-keeping protein GAPDH, used as loading control. (*d*) Immunoprecipitation of Raf-1 with anti-Raf-1 rabbit polyclonal and subsequent probing with Bcl-2 mAb antiserum as described in "Material and methods". Under the same experimental conditions, both Raf-1 (*e*) and Bcl-2 (*f*) expression was also evaluated through Western blotting using specific anti-Raf-1 and anti-Bcl-2 specific Mabs, respectively, as described in Material and methods. (*g*) Band intensities associated to pErks and Raf-1/Bcl-2 complexes. The intensities of the bands are expressed in arbitrary units. Bars, SDs. Asterisks indicate the statistical significance of data ($p < 0.005$). Lipo, KB cells treated with lipofectamine without plasmid; C4, KB cells transfected with dominant negative RSV-Raf-C4; BXB, KB cells transfected with dominant positive (DP) RSV-Raf-BXB; CTR, untreated; FTI, 48 hr 0.07 μM R115777; IFNα, 48 hr 500 IU/ml IFNα; IFNα + FTI, 48 hr 500 IU/ml IFNα + 0.07 μM R115777. The cells were also processed for the determination of the phosphorylation (*h*) and expression (*i*) of Bad evaluated after blotting with specific antibodies, as described in "Material and methods". (*j*) Expression of the house-keeping protein GAPDH, used as loading control. CTR, untreated; FTI, 48 hr 0.07 μM R115777; IFNα, 48 hr 500 IU/ml IFNα; IFNα + FTI, 48 hr 500 IU/ml IFNα + 0.07 μM R115777. The experiments were performed at least 3 different times and the results were always comparable.

tion with a constitutively active Raf-1 (Fig. 7*a*). Both R115777 and the combined treatment induced a significant decrease of Erk activity (83 and 86% of control, respectively) (Figs. 7*a* and 7*g*). All the treatments had no effects on the expression of these enzymes (Fig. 7*b*). Subsequently, Raf-1 was immunoprecipitated, run on PAGE and electrotransferred on nitrocellulose film that was immunoblotted for bcl-2 (Fig. 7*d*). We have found that IFNα induced an increase of the immuno-conjugate formation between Raf-1 and bcl-2 (180% of control) while R115777 alone caused a significant reduction of the co-immunoprecipitated in parental cells (40% of control) (Figs. 7*d* and 7*g*). In the same experimental conditions, R115777 was able to antagonize the increase of immuno-conjugate formation induced by IFNα (98% of control) (Figs. 7*d* and 7*g*). The transfection of KB cells with DN Raf-1 caused co-immunoprecipitate reduction (55% of control) that was again restored by IFNα (102% of control) (Figs. 7*d* and 7*g*). The restoring effect of IFNα was again antagonized by R115777 (41% of control) that alone induced only a slight decrease of the immunoconjugate formation (32% of control) (Figs. 7*d* and 7*g*). The DP Raf-1 transfection caused a significant increase of Raf-1/bcl-2 immunoconjugates (141% of control) that was antagonized by the exposure of the cells to R115777 alone (64% of control) while IFNα did not change Raf-1/bcl-2 interaction (138% of control) (Figs. 7*d* and 7*g*). On the other hand, the combination between the 2 agents antagonized the conjugate formation increase induced by the transfection (35% of control) (Figs. 7*d* and 7*g*). Both total bcl-2 and raf-1 expression were almost unchanged by the different treatments (Figs. 7*e* and 7*f*, respectively). Interestingly, the transfection with the DN Raf-1 sensitized KB cells to the antiproliferative activity of IFNα since an about 72% of growth inhibition was recorded. In these experimental conditions, the combination did not increase the growth inhibition. On the other hand, the transfection with DP Raf-1 reduced the activity of IFNα since only 25% of growth inhibition was found. The combination caused an about 80% of growth inhibition thus potentiating the effects induced by the cytokine alone (data not shown).

Subsequently, we have examined the effects of IFNα and R115777 on the phosphorylation in ser 112 of Bad. IFNα increased the phosphorylation of Bad and again R115777 completely antagonized this effect while the R115777 alone had no effect (Fig. 7*h*). These findings occurred without changes in the expression of total Bad (Fig. 7*i*). The interaction between bcl-2 and Raf-1 was also confirmed by confocal microscopy (Fig. 8). In fact, in untreated cells, the 2 proteins partially co-localized in the cytoplasm and the co-localization was significantly increased by the treatment with IFNα for 48 hr (Figs. 8*a*–8*c* and 8*g*–8*i*, respectively). On the other hand, the treatment of KB cells with R115777 alone for 48 hr reduced bcl-2/Raf-1 co-localization (Figs. 8*d*–8*f*). The treatment of KB cells with R115777 for 48 hr completely antagonized the increase of Raf-1/bcl-2 co-localization induced by IFNα (Figs. 8*j*–8*l*).

Discussion

In this paper we have investigated whether the inhibition of the activity of Ras with the use of the FTI R115777 (Zarnestra) could strengthen both growth inhibition and apoptosis induced by IFNα in human epidermoid cancer cells. In detail, cell growth assays performed *in vitro* showed a clear synergistic antiproliferative effect as demonstrated by the median drug effect analysis and by the derived CIs. In fact, IFNα and FTI given in combination were strongly synergistic since a CI_{50} less than 0.5 was recorded. Moreover, IFNα/R115777 combination lowered the active concentrations of both drugs at *in vivo* achievable therapeutic concentrations (0.1 μM range for R115777 and 500 IU/ml for IFNα). Interestingly, higher PFs for R115777 were recorded when the 2 drugs were used at the following molar ratio: IFNα/R115777 = 75:25. In other words, the combination was highly synergistic when

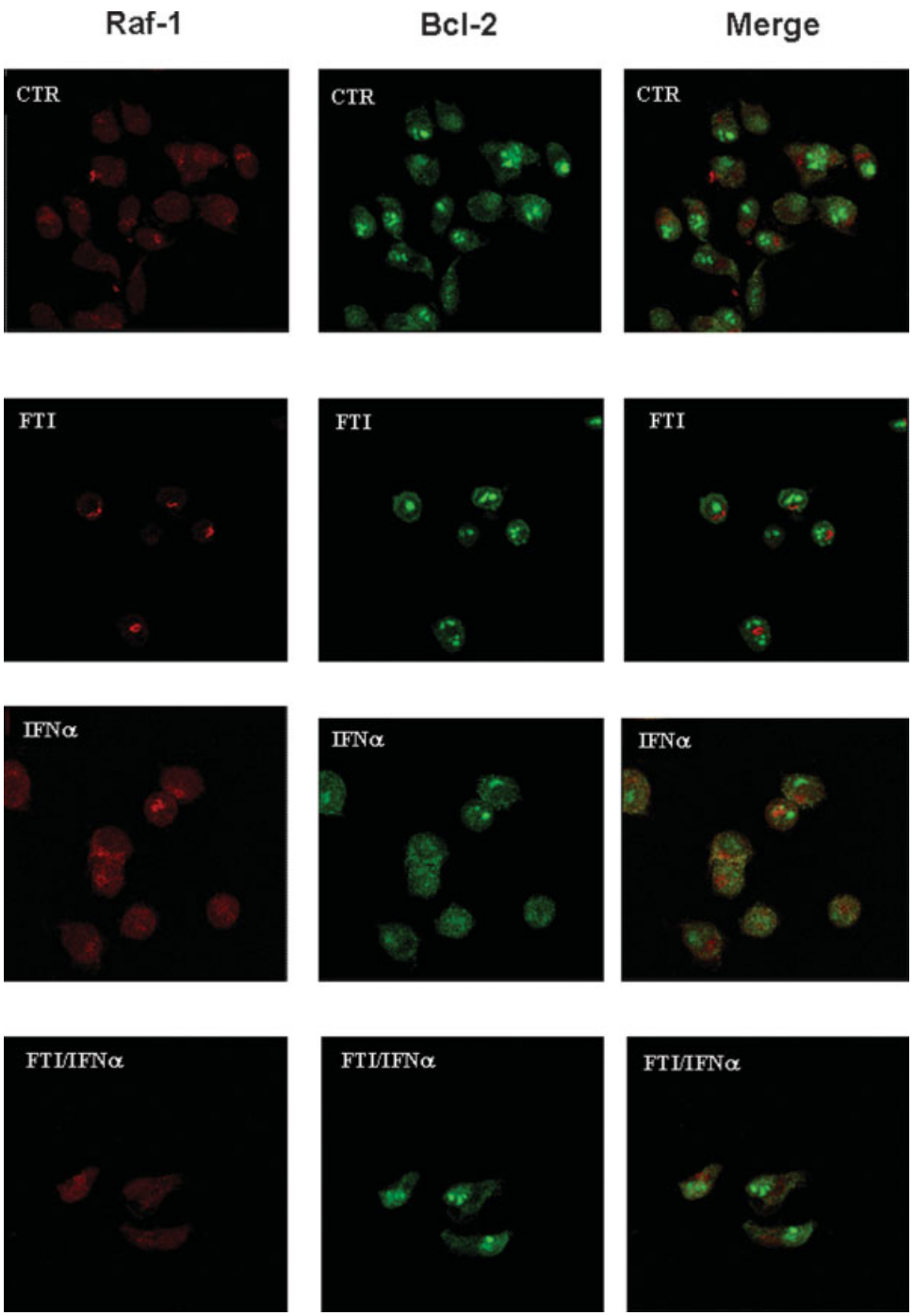

FIGURE 8 – Co-localization of Bcl-2 and Raf-1 in KB cells. KB cells were treated with 500 IU/ml IFNα and/or 0.07 μM for 48 hr and processed for the visualization of Bcl-2 and Raf-1 at confocal microscopy as described in "Material and methods". Raf-1: Raf-1 immuno-visualization; Bcl-2: Bcl-2 immuno-visualization; Merge: fluorescence overlapping. CTR, untreated; FTI, 48 hr 0.07 μM R115777; IFNα, 48 hr 500 IU/ml IFNα; IFNα + FTI, 48 hr 500 IU/ml IFNα + 0.07 μM R115777. The experiments were performed at least 3 different times and the results were always comparable.

higher concentrations of IFNα were used. Clinical settings, in our opinion, should take advantage of our preclinical data since the combination allows lowering the active dosages of R115777 while IFNα concentrations maintain similar to those used in the single administration. This could have several advantages in reducing the side effects caused by R115777 administration (myelosuppression, neurological and gastrointestinal side effects) preserving R115777 antitumor activity. A possible mechanistic explanation of this effect could be the following: higher dosages of IFNα were required in order to induce the over-activation of the EGF-Ras-dependent survival pathway that made tumor cells more sensitive to the ras-inhibitory strategies. Moreover, the concentrations of drugs used in the combination for *in vivo* studies were lower than those are used to achieve therapeutic effects. Finally, a pro-apoptotic enhance of the effects of the 2 drugs was also observed in the same experimental conditions.

Since it has been reported that FTIs can induce apoptosis in tumor cells through the induction of the expression of the death domain receptor Fas we have investigated if the synergistic effects on apoptosis induced by the combination between R115777 and IFNα were paralleled by Fas expression increase.[32] However, IFNα neither alone nor in combination was able to increase the surface Fas expression in this experimental model.

We have also found that the treatment of KB cells with IFNα alone for 48 hr induced an increase of Ras activity in the absence of changes in its expression while R115777 at low doses caused only a slight decrease of Ras activity. However, R115777 completely antagonized the effect of IFNα when used in combination with the cytokine. The impairment of Ras activity induced by the combined treatment was paralleled by a reduced stimulation of both the downstream Erk and Akt survival enzymes. These data suggest that the synergistic growth inhibitory and pro-apoptotic effects produced by the IFNα/FTI combination involved the inhibition of both Erk and Akt survival pathways acting in these cells in a Ras-dependent fashion. We cannot exclude in our experimental model a direct interaction between components of the IFNα-mediated pathway (*i.e.* STAT1) and Erk1-2 as previously reported by Darnell *et al*.[35] We have found a cooperative antitumor effect of IFNα and R115777 combination *in vivo* on nude mice xenografted with KB cells. As previously demonstrated *in vitro*, the combination induced also *in vivo* enhanced apoptosis and antagonism on the IFNα-induced hyper-activation of Ras and its terminal enzyme Erk. On the other hand, R115777 did not counteract the increase of EGF-R activation induced by IFNα; in fact, FTI R115777 acts on ras that is a target downstream to EGF-R. These data suggested that the *in vivo* cooperative effect between the 2 agents depended upon the disruption of the Ras-mediated survival pathways elicited by the cytokine. On the basis of these results we have further investigated on the molecular mechanisms of the antiapoptotic effects of the Ras-dependent pathway elicited by IFNα in this experimental model. We have previously demonstrated that the hyper-activation of the EGF-Ras-dependent pathway by IFNα increases the activity of the downstream targets Raf-1 and Erk.[17] Raf-1 is a serine/threonine kinase that stimulates phosphorylation of the pro-apoptotic protein Bad. In other cell systems, plasma membrane targeting of Raf-1 activates the classical MEK1/Erk (MAPK) cascade but does not protect cells, whereas mitochondrial targeting of Raf-1 protects cells from apoptosis.[36] The antiapoptotic signals from Raf-1 can be either MEK-independent or MEK-dependent, the latter through a MEK/Erk/ribosomal S6 kinase cascade.[37] The MEK-independent signal is not well defined, and additional studies are required for solving the role of Raf-1 in Bad phosphorylation.[24,36,38]

Bcl-2 is the strongest candidate for the mitochondrial targeting of Raf-1 because it was shown that Bcl-2 knock down by interference reduced Raf-1 mitochondrial localization.[33] Therefore, Raf-1 translocation to mitochondria could displace Bcl-2 from Bad, activating the antiapoptotic activity of the former. Moreover, it has been demonstrated that Raf-1 co-immunoprecipitates with Bcl-2 in several experimental models.[39] On the basis of these results, we have investigated whether IFNα could increase the *in vitro* interaction between Raf-1 and Bcl-2 and induce the targeting of Raf-1 to mitochondria. We have demonstrated that IFNα indeed increases Raf-1/Bcl-2 interactions both in co-immunoprecipitation and intracellular co-localization experiments and enhances Bad phosphorylation. At the same experimental conditions, translocation of Raf-1 to mitochondria was also recorded. All these effects were antagonized by the concomitant treatment of KB cells with R115777 and IFNα, suggesting that the Ras-dependent survival pathway involved the interaction of Raf-1 with Bcl-2 and the consequent displacement of Bad from Bcl-2 thus activating the antiapoptotic function of the latter. Moreover, the use of plasmids encoding for DN or DP Raf-1 antagonized and potentiated, respectively, the co-immunoprecipitation between Raf-1 and Bcl-2, suggesting that this effect was specifically due to the over-activation of Raf-1 induced by IFNα. Interestingly, the transfection with either the DN or DP Raf-1 strongly modulated the activity of Erk-1 and 2, suggesting that Raf-1 has a critical role in the regulation of this pathway in this experimental model. These data agreed with our recent findings that demonstrate the activation of a mitochondrial pathway that is completely antagonized by exposure to EGF in IFNα-treated epidermoid cancer cells.[40]

In conclusions, we have demonstrated that IFNα elicits a survival response in human epidermoid cancer cells, mediated by ras and abrogated by the FTI R115777 both *in vitro* and *in vivo*. These findings offer the rationale for the study of this therapeutic combination in the clinical setting.

The data reported here on the molecular correlates of this effect as well as the findings from previous studies[17,19] indicate that the Ras-Raf-1-dependent pathway has a pivotal role in these effects. We also provide the first experimental evidence that IFNα induces a survival pathway that involves interaction of Raf-1 with Bcl-2, Raf-1 translocation to the nucleus, phosphorylation of Bad and displacement of the latter from Bcl-2. R115777 suppress all these processes opening a new scenario of anticancer intervention in order to strengthen the antitumor activity of IFNα.

Acknowledgements

We thank Dr. Alessandro Ottaiano for his support in the statistical elaboration of the data. This work was partially supported by PRIN 2005 (MIUR Rome) to A.A. and by Associazione Italiana Ricerca sul Cancro (AIRC) to M.C. and grants from Italian Ministry of Health to A.B. (FSN 2004) and M.C. (FSN 2005). Dr. Giuseppina Meo was supported by a grant from the Centro Regionale di Competenza di "Diagnostica e Farmaceutica Molecolari" of Regione Campania. This manuscript is dedicated to the beloved memory of Salvatore Venuta.

References

1. End DW, Smets G, Todd AV, Applegate TL, Fuery CJ, Angibaud P, Venet M, Sanz G, Poignet H, Skrzat S, Devine A, Wouters W, et al. Characterization of the antitumour effects of the selective farnesyl protein transferase inhibitor R115777 in vivo and in vitro. Clin Cancer Res 2001;7:3544–50.
2. End DW. Farnesyl protein transferase inhibitors and other therapies targeting the Ras signal transduction pathway. Invest New Drugs 1999;17:241–58.
3. Mesa RA. Tipifarnib: farnesyl transferase inhibition at a crossroads. Expert Rev Anticancer Ther 2006;10:313–19.
4. Kelland LR, Smith V, Valenti M, Patterson L, Clarke PA, Detre S, End D, Howes AJ, Dowsett M, Workman P, Johnston SR. Preclinical antitumour activity and pharmacodynamic studies with the farnesyl protein transferase inhibitor R115777 in human breast cancer. Clin Cancer Res 2001;7:3544–50.
5. Budillon A, Tagliaferri P, Caraglia M, Torrisi MR, Normanno N, Iacobelli S, Palmieri G, Stoppelli MP, Frati L, Bianco AR. Upregulation of epidermal growth factor receptor induced by α-interferon in human epidermoid cancer cells. Cancer Res 1991;51:1294–9.
6. Selleri C, Maciejewski JP, Montuori N, Ricci P, Visconte V, Serio B, Luciano L, Rotoli B. Involvement of nitric oxide in farnesyltransferase inhibitor-mediated apoptosis in chronic myeloid leukemia cells. Blood 2003;102:1490–1498.
7. Clark-Lewis I, Sanghera JS, Pelech SL. Definition of a consensus sequence for peptide substrate recognition by p44mpk: the meiosis-activated myelin basic protein kinase. J Biol Chem 1991;266:15180–4.
8. Shields JM, Pruitt K, Mc Fall A, Shaub A, Der CJ. Understanding Ras: 'it ain't over 'til it's over'. Trends Cell Biol 2000;10:147–54.

9. Gullick WJ, Marsden JJ, Whittle N. Expression of epidermal growth factor receptors on human cervical ovarian and vulval carcinomas. Cancer Res 1986;46:285–92.
10. Foncea R, Galvez A, Perez V, Morales MP, Calixto A, Melendez J, Gonzalez-Jara F, Diaz-Araya G, Sapag-Hagar M, Sugden PH, LeRoith D, Lavandero S. Extracellular regulated kinase, but not protein kinase C, is an antiapoptotic signal of insulin-like growth factor-1 on cultured cardiac myocytes. Biochem Biophys Res Commun 2000; 273:736–44.
11. Kang C, Yoo S, Hwang B, Kim KW, Kim DW, Kim CM, Kim SH, Chung BS. The inhibition of ERK/MAPK not the activation of JNK/SAPK is primarily required to induce apoptosis in chronic myelogenous leukemic K562 cells. Leuk Res 2000;24:527–34.
12. Jan MS, Liu HS, Lin YS. Bad overexpression sensitizes NIH/3T3 cells to undergo apoptosis which involves caspase activation and ERK inactivation. Biochem Biophys Res Commun 1999;264: 724–9.
13. Nunez G, Benedict MA, Hu Y, Inohara N. Caspases: the proteases of the apoptotic pathway. Oncogene 1998;17:3237–45.
14. Thyrell L, Erickson S, Zhivotovsky B, Pokrovskaja K, Sangfelt O, Castro J, Einhorn S, Grander D. Mechanisms of Interferon-α induced apoptosis in malignant cells. Oncogene 2002;21:1251–62.
15. Caraglia M, Pinto A, Correale P, Zagonel V, Genua G, Leardi A, Pepe S, Bianco AR, Tagliaferri P. 5-Aza-2′-deoxycytidine induces growth inhibition and upregulation of epidermal growth factor receptor on human epithelial cancer cells. Ann Oncol 1994;5:269–76.
16. Budillon A, Di Gennaro E, Caraglia M, Barbarulo D, Abbruzzese A Tagliaferri P. 8-Cl-cAMP antagonizes mitogen-activated protein kinase activation and cell growth stimulation induced by epidermal growth factor. Br J Cancer 1999;81:1134–41.
17. Caraglia M, Tagliaferri P, Marra M, Giuberti G, Budillon A, Gennaro ED, Pepe S, Vitale G, Improta S, Tassone P, Venuta S, Bianco AR, et al. EGF activates an inducible survival response via the RAS → Erk-1/2 pathway to counteract interferon-α-mediated apoptosis in epidermoid cancer cells. Cell Death Differ 2003;10:218–29.
18. Tagliaferri P, Caraglia M, Muraro R, Budillon A, Pinto A, Bianco AR. Pharmacological modulation of peptide growth factor receptor expression on tumour cells as a basis for cancer therapy. Anticancer Drugs 1994;5:379–93.
19. Caraglia M, Abbruzzese A, Leardi A, Pepe S, Budillon A, Baldassare G, Selleri C, Lorenzo SD, Fabbrocini A, Giuberti G, Vitale G, Lupoli G, et al. Interferon-α induces apoptosis in human KB cells through a stress-dependent mitogen activated protein kinase pathway that is antagonized by epidermal growth factor. Cell Death Differ 1999; 6:773–80.
20. Widmann C, Gibson S, Jarpe MB, Johnson GL. Mitogen-activated protein kinase: conservation of a three-kinase module from yeast to human. Physiol Rev 1999;79:143–80.
21. Garrington TP, Johnson GL. Organization and regulation of mitogen-activated protein kinase signaling pathways. Curr Opin Cell Biol 1999;11:211–18.
22. Yan CYI, Greene LA. Prevention of PC12 cell death by *N*-acetylcysteine requires activation of the Ras pathway. J Neurosi 1998; 18:4042–9.
23. Aikawa R, Komuro I, Yamazaki T, Zou Y, Kudoh S, Tanaka M, Shiojima I, Hiroi Y, Yazaki Y. Oxidative stress activates extracellular signal-regulated kinases through Src and Ras in cultured cardiac myocytes of neonatal rats. J Clin Invest 1997;100:1813–21.
24. von Gise A, Lorenz P, Wellbrock C, Hemmings B, Berberich-Siebelt F, Rapp UR, Troppmair J. Apoptosis suppression by Raf-1 and MEK1 requires MEK- and phosphatidylinositol 3-kinase-dependent signals. J Mol Cell Biol 2001;21:2324–36.
25. Zhou H, Li XM, Meinkoth J, Pittman RN. Akt regulates cell survival and apoptosis at a postmitochondrial level. J Cell Biol 2000;151:483–94.
26. Bruder JT, Heidecker G, Rapp UR. Serum-, TPA-, and. Ras-induced expression from. Ap-1/Ets-driven promoters requires. Raf-1 kinase. Genes Dev 1992;6:545–56.
27. Chou TC, Motzer RJ, Tong Y, Bosl GJ. Computerized quantitation of synergism and antagonism of taxol, topotecan, and cisplatin against human teratocarcinoma cell growth: a rational approach to clinical protocol design. J Natl Cancer Inst 1994;86:1517–24.
28. Magne N, Fischel JL, Dubreuil A, Formento P, Marcie S, Lagrange JL, Milano G. Sequence-dependent effects of ZD1839 ('Iressa') in combination with cytotoxic treatment in human head and neck cancer. Br J Cancer 2002;86:819–27.
29. Solorzano CC, Hwang R, Baker CH, Bucana CD, Pisters PW, Evans DB, Killion JJ, Fidler IJ. Administration of optimal biological dose and schedule of interferon α combined with gemcitabine induces apoptosis in tumor-associated endothelial cells and reduces growth of human pancreatic carcinoma implanted orthotopically in nude mice. Clin Cancer Res 2003;9:1858–67.
30. Sommer K, Peters SO, Robins IH, Raap M, Wiedemann GJ, Remmert S, Sieg P, Bittner C, Feyerabend T. A preclinical model for experimental chemotherapy of human head and neck cancer. Int J Oncology 2001;18:1145–9.
31. Teicher BA. In vivo tumour response end points. In: Teicher BA, ed. Tumour models in cancer research. Totowa, NJ: Humana Press, 2002. 593–616.
32. Zhang B, Prendergast GC, Fenton RG. Farnesyltransferase inhibitors reverse Ras-mediated inhibition of Fas gene expression. Cancer Res 2002;62:450–8.
33. Caraglia M, Budillon A, Tagliaferri P, Marra M, Abbruzzese A, Caponigro F. Isoprenylation of intracellular proteins as a new target for the therapy of human neoplasms: preclinical and clinical implications. Curr Drug Targets 2005;6:301–23.
34. Jin S, Zhuo Y, Guo W, Field J. p21-activated Kinase 1 (Pak1)-dependent phosphorylation of Raf-1 regulates its mitochondrial localization, phosphorylation of BAD, and Bcl-2 association. J Biol Chem 2005;280:24698–705.
35. Darnell JE, Jr, Kerr IM, Stark GR. Jak-STAT pathways and transcriptional activation in response to IFNs and other extracellular signaling proteins. Science 1994;264:1415–21.
36. Wang H, Rapp U, Reed JC. Bcl-2 targets the protein kinase Raf-1 to mitochondria. Cell 1996;87:629–38.
37. Baccarini M. An old kinase on a new path. Raf and apoptosis. Cell Death Differ 2002;9:783–5.
38. Hindley A, Kolch W. Extracellular signal regulated kinase (ERK)/mitogen activated protein kinase (MAPK)-independent functions of Raf kinases. J Cell Sci 2002;115:1575–81.
39. Kerkhoff E, Rapp UR. Cell cycle targets of Ras/Raf signalling. Oncogene 1998;17:457–62.
40. Boccellino M, Giuberti G, Quagliuolo L, Marra M, D'Alessandro AM, Fujita H, Giovane A, Abbruzzese A, Caraglia M. Apoptosis induced by interferon-α and antagonized by EGF is regulated by caspase-3-mediated cleavage of gelsolin in human epidermoid cancer cells. J Cell Physiol 2004;201:71–83.